Identifying Mutational Hotspots using Differences in Atomic Fluctuations combined with Positional Variability

***Elvis A. F. Martis*[†]* *and Evans C. Coutinho*[†#]**

[†]Molecular Simulations Group, Department of Pharmaceutical Chemistry, Bombay College of Pharmacy, Kalina, Santacruz [E], Mumbai 400098, India.

[#]St John Institute of Pharmacy and Research, Vevoor, Manor Road, Palghar East, District Palghar 401404

*Author for correspondence

ABSTRACT

Amino acid substitutions in proteins resulting from gene mutations are essential to the evolutionary process that enhances the organism's adaption and survival rate. The primary aim of such substitution is to improve the protein's function and structural stability. Various computational and experimental techniques are available to understand the effect of amino acid substitution on a protein's function and structural stability and ultimately the effect on drug binding. This work seeks to understand how amino acid substitutions help overcome the anti-infective effect of drugs by diminishing their inhibitory potential. We attempt to locate hotspots among the amino acids in the binding site, where substitutions are likely to cause drug resistance. To achieve this, we propose an empirical score using atomic fluctuations coupled with amino acid variability to identify amino acids that are likely to mutate, leading to drug resistance. The scoring method has been developed and validated on two extensively studied drugs inhibiting HIV-1 protease, namely nelfinavir and darunavir. Further, we choose anaplastic lymphoma kinase (ALK) and its inhibitor, crizotinib, to test the performance of this empirical score. The prediction works well for amino acids within a radius of 5 Å from the centre of mass of the drug. The advantage of this method is that it is computationally inexpensive compared to free energy-based methods. However, we note that the predictions are not consistent for amino acids that are outside the active site, and there are no provisions in the methodology at this moment to address double or triple mutants.

KEYWORDS

Drug resistance, molecular dynamics simulations, atomic fluctuations, amino acid variability, HIV-1 protease, anaplastic lymphoma kinase.

INTRODUCTION

Drug-induced selection pressure(1–3) drives the evolution of infectious organisms or cancer cells in the direction of reduced drug sensitivity. The organisms or cells adapt to overcome the effect of drugs by one or more mechanisms. As a defence mechanism against drugs, the organism can down-regulate the expression of influx channels/pumps that enable the entry of the drug into the cell. This results in a decreased concentration within the cell. Another adaptation that hinders the build-up of the drug inside the cell is the upregulation of the expression of efflux channels/pumps that facilitate the egress of the drug. These processes are modulated by complicated pathways involved in the upregulation or downregulation of various proteins that regulate the traffic to and from the cell. Because of the complications, this area is the least studied by computational techniques based on atomistic simulations and free energy calculations. Target site substitutions(4,5) that lead to disruption in drug binding without significant loss of protein function(6,7) is another mechanism that leads to drug resistance. Such substitutions have been extensively studied using computer simulations that can estimate the difference in the drug's affinity to the mutant and the wild-type protein. Enzymes in biochemical pathways undergo substitutions that improve the survival rate of the organism. This can involve either improving the protein function through catalytic efficiency and stability (accessory mutations) or escaping the inhibitory action of drug molecules (major mutations). In the latter case, the driving force for modification of the drug target is disruption of drug binding, while leaving substrate binding unperturbed. Most computational methods employed to study the mechanism of drug resistance, attempt to understand the differences in the binding patterns of the substrate and the drug molecule, also referred to as the substrate envelope hypothesis(8–10).

In current literature(11,12) two main classes of methods may be found that are used to predict/study drug-resistant mutations. The first class comprises sequence-based methods and the second class, the structure-based methods. Much of the structure-based methods used to study drug resistance attempt to compute the change in the binding free-energy of the drug upon mutation[8]. Methods used to compute the absolute free energy of binding are computationally very demanding compared to methods used to compute the relative free energy change on binding. The method described in this work belongs to the structure-based class of methods, however, we do away with the need to compute the change in the free energy of binding which is savings in time and computational cost. The main theme of the method presented here is that it examines binding-site positions with MD simulations carried out on three different states, namely, the *apo* state, the substrate-bound state, and the drug-bound state. The amino acid residues crucial for binding are identified based on the changes in their atomic fluctuations in the presence of the substrate and/or the drug. Moreover, the product of the change in the atomic fluctuations and the amino acid sequence variability, identifies amino acids amenable to mutations. Furthermore, a multiple sequence alignment identifies amino acid substitutions that are likely to be tolerated at a given position. This method is largely motivated by an idea reported by Kollman *et al*(13,14). However, the current method differs in two ways; first, the use of the energy component of binding free energy reported by Kollman *et al.* is replaced by the change in the atomic fluctuations, and secondly, the more reliable Hidden Markov Model (HMM) is used for multiple sequence alignment to improve the identification of remotely homologous proteins.

METHODS

Preparation of systems for molecular dynamics simulation

The coordinates for the protein-ligand complexes were retrieved from the Protein Data Bank (PDB); the PDB entries used in this study are listed in **Table S1** in the supplementary information. The X-ray structures were imported and processed in the Maestro-GUI (Schrödinger suite, 2018). All systems were prepared for MD simulations with the *Leap* module in AMBERtools15. Protein atoms were atom-typed according to the AMBER14 (ff14SB) force field.

Generating AMBER-compatible parameters for ligands

All ligands, except ATP, were optimized in vacuum using Gaussian03(15) at the density functional level of theory (DFT) with the B3LYP hybrid functional and the 6-311G^{++}(d, p) basis set. These geometries were used to compute the electrostatic potentials (ESPs) by the Merz-Kollman scheme(16). To fit the partial charges to the ESPs, the Restrained Electrostatic Potential (RESP) method implemented in *Antechamber*(17) and *parmchk* in AMBERtools15 was used. The General AMBER force field(18) (GAFF) was used to define the atom types, atomic masses, and force constants for bonds, angles, torsions, and improper torsions. All force field parameters for ATP were adopted as defined by Carlson *et al*(19).

Preparing the initial configuration of HIV-1 protease

All mutations induced for stability for crystallographic purposes were reverted to the wild-type amino acid. The substrate for HIV-1 protease considered in this work is the CA-p2 fragment (sequence - KARVLAEAMS). The catalytically inactive D25N mutation was also reverted to

the wild-type amino acid. The protonation states of the catalytically important D25 and D25′ residues were adopted as reported by Wright *et al*(20).

Preparing the initial configuration of human anaplastic lymphoma kinase (ALK)

In the X-ray crystal structures of human anaplastic lymphoma kinase (PDB id 2XP2 and 3LCT), coordinates have not been reported for amino acid residues from L1122 to E1129. To correct this, Modeller's loop refinement tool in the Chimera-GUI(21) was used to predict the missing loop. ATP was built by adding a phosphate group to the coordinates of ADP (PDB id 3LCT). The initial configuration for the *apo*protein was built by deleting the ADP molecule from 3LCT (PDB id).

Molecular dynamics simulations

All complexes were solvated with TIP3P waters(22) enclosed in a box with dimensions extending 12 Å beyond any protein atom, and an appropriate number of neutralizing ions were added to maintain the neutrality of the system. The complexes were relaxed using three cycles of minimization of 50,000 steps each. The first 10,000 steps of minimization adopted the steepest descent algorithm, and the remaining 40,000 steps used the conjugate gradient algorithm. The cut-off for evaluating non-bonded interactions was placed at 8.0 Å for the minimization phase. The first cycle of minimization was performed with 25 kcal/(mol $Å^2$) restraining force on the solute atoms, this force constant was reduced to 5 kcal/(mol $Å^2$) in the next cycle, and the final cycle was performed without any restraining forces on either the solute or the solvent atoms. The system was heated from 0 K to 300 K for 1 ns with 5 kcal/(mol $Å^2$) restraining force on the solute atoms using the Langevin dynamics, with a collisional frequency of 2 ps^{-1}. After heating, the system was equilibrated by MD simulations under the NVT

ensemble for six cycles of 1 ns each, where the restraining force on the solute atoms was gradually reduced from 5.0 to 0.0 kcal/(mol $Å^2$). The next step employed the NPT ensemble for density equilibration for another six cycles of 1 ns each, with the restraining force on the solute atoms gradually decreasing from 5 to 0 kcal/(mol $Å^2$). In the equilibration phase, the cut-off for evaluating non-bonded interactions was placed at 9 Å. In the production phase of the MD simulations, all systems were simulated for 100 ns in triplicate, amounting to a 300 ns trajectory for each system. The long-range electrostatic interactions were calculated using the Particle Mesh Ewald (PME) summation method(23). The minimization and equilibration phases of MD simulations were carried out with the MPI version of the *SANDER* and *PMEMD* codes implemented in AMBER14(24), respectively. The production phase was carried out using the CUDA-enabled code of *PMEMD* in AMBER14. All simulations were performed with the SHAKE(25) algorithm to constrain bonds to hydrogen atoms, with the tolerance set to 0.00001 Å. A 2-fs integration time step was used to solve Newton's equations of motion. For analysis, the conformations were saved every 100 ps, amounting to 1000 snapshots per trajectory (3000 per system).

Analysis of MD trajectory

Analysis of the MD trajectory was performed with the *Cpptraj*(26) module in AMBERTools15. Before the analysis, all solvent atoms and neutralizing ions were stripped off, and the protein conformations were aligned to the first frame. The mass-weighted Cα root-mean-square deviation (RMSD) for the protein was computed using the X-ray conformation as the reference. The convergence of MD trajectories was estimated using the root-mean-squared average correlation (RAC) with mass-weighted RMS averaging of Cα atoms, with the first frame of the

trajectory as the reference. The root-mean-square fluctuations (RMSF) per residue for the backbone and side-chain atoms were computed from the last 50 ns part of the trajectories.

Computing amino acid variability and ΔFV score.

The gapped multiple sequence alignment (MSA) to compute the amino acid variability was generated using the program *HHBLITS*(27). *HHBLITS* uses Hidden Markov Models (HHM) to search for remote homologous proteins. The E-value was set to 0.0001, a maximum of 8 iterations was performed, and the UNICLUST30(28) database (default) was used to search for homologous proteins. The MSAs were imported into *Bioedit* (biological sequence editor) to compute the amino acid variability at each position. In this work, the Wu-Kabat variability coefficient(29) (**Eq 1**) was computed at each position to measure the positional variability.

$$(\text{Wu} - \text{Kabat variability coefficient})^{i} = \frac{(N * k^{i})}{n^{i}} \qquad \textbf{Eq 1}$$

where N is the total number of sequences aligned, k^i is the number of different types of amino acids found to substitute the wild-type amino acid at the ith position (gaps excluded), and n^i is the number of times the wild-type amino acid occurs at the ith position. The Wu-Kabat coefficient of variability considers the number of different types of amino acids that substitute the wild-type residue along with the frequency of occurrences of the wild-type amino acid residue. Therefore, if the wild-type amino acid is not well conserved, for example, if it occurs less than 50%, and the remaining 19 amino acids are found to substitute the wild-type, then Wu-Kabat's coefficient of variability takes a large number.

The sequences for all the drug targets used in this work were imported from the UniProt database(30). For HIV-1 protease, the UniProt accession number is Q9Q288, and for human

anaplastic lymphoma kinase (ALK), it is Q9UM73 (residues 1093-1400; the kinase domain on which the study has been carried out).

The ΔFV score (*F*luctuation and *V*ariability) is an empirical score that equals the product of the amino acid sequence variability and the difference in atomic fluctuation (ΔRMSF). ΔFV_1 (**Eq 2a**) is obtained by taking the difference of the atomic fluctuations for the amino acid at the ith position in the *apo*protein and the amino acid in the *holo*protein bound with either the substrate or the drug. A second fluctuation score ΔFV_2 (**Eq 2b**) is also computed by taking the difference of atomic fluctuation for the amino acid at the ith position in the substrate-bound protein and the drug-bound protein. The difference in the ΔFV_1 and ΔFV_2 scores is subtle: on the face of it, both scores identify the impact of the binding of a small molecule on the protein mobility weighted by the positional variability of an amino acid. However, the latter score identifies amino acid positions that show more pronounced interactions with the drug than the substrate, and therefore, are more likely to mutate with minimal effect on the protein function(13) (*vide infra*).

$$\Delta FV_1^i = \Delta RMSF^i_{(\text{apo} - \text{drug or substrate})} * (\text{Wu} - \text{Kabat variability coefficient})^i \qquad \textbf{Eq 2a}$$

$$\Delta FV_2^i = \Delta RMSF^i_{(\text{substrate} - \text{drug})} * (\text{Wu} - \text{Kabat variability coefficient})^i \qquad \textbf{Eq 2b}$$

where $\Delta RMSF^i$ is the difference in atomic fluctuations at the ith position in the amino acid sequence.

RESULTS AND DISCUSSION

The method described in this work to identify mutational hotspots is fast and simple such that it can routinely be incorporated as a drug-resistance screen in the drug discovery process. The scoring method was first tested on HIV-1 protease inhibitors (viz., nelfinavir and darunavir) whose effects have been measured on clinically observed resistance cases. After satisfactory performance the method was used to predict mutations likely to be observed for anaplastic lymphoma kinase by the inhibitor crizotinib. As for structure-based methods that have been applied to study drug resistance, this method can be applied to situations where there is no *a priori* knowledge of drug-resistant mutations. The method can identify residues that are critical for both substrate and drug binding. This information can be harnessed to develop inhibitors that demonstrate strong interactions with residues that lie within the substrate envelope; with lower chances of developing resistance(31–33) in the future.

Equilibration of MD trajectories

It is of paramount importance that atomic fluctuations are extracted from the well-equilibrated part of the MD trajectories. The Cα-RMSD and RAC (**Figures S1-S4** in supplementary information) were computed to monitor the equilibration of MD trajectories. The maximum in the normalized distribution for Cα-RMSD for all trajectories is seen between ~1.0-2.0 Å. This indicates that the MD-generated conformations do not deviate drastically from their X-ray conformations. Moreover, we also employ RAC, an additional method to evaluate the equilibration of MD trajectories. The rate at which RAC decays suggests the speed at which a system would achieve dynamic equilibrium(34,35). **Figures S3** and **S4** suggest that RAC tends to decay fast, and after ~50 ns the RAC values are less than ~0.6 Å. Moreover, most of the

structural adjustments are seen in the initial parts of the trajectories around ~10-30 ns. Therefore, all per-residue atomic fluctuations were obtained from the last 50 ns of the MD trajectories.

Significance of the ΔFV scores

It is well-established that drug-resistant mutations are more likely to occur at positions that are not well conserved and those that show more pronounced interactions with the drug than with the substrate or the natural ligand(13). This ensures minimal or no fitness costs. However, mutations are not uncommon at positions that interact more strongly with the substrate, where the mutation is likely to result in an enhanced catalytic efficiency or protein function. Some mutations reduce protein function or catalytic efficiency. The likelihood of these mutations propagating in future generations will depend on the balance between the fitness penalty and the magnitude of the drug-induced selection pressure. To overcome the fitness cost, compensatory or gain-of-function mutations are known to salvage the protein's lost functions.

We attempt to capture these aspects quantitatively using the ΔFV scores and to locate amino acids where mutations are more likely to be seen causing drug resistance. To understand how drug binding alters atomic fluctuations in the amino acid residues in the wild-type enzyme vis-à-vis the substrate, molecular dynamics simulations for both *apo*- and *holo*-forms were performed in an explicit water box for a sufficiently long time. The drug targets employed here were simulated under three conditions, first, when the binding site is unoccupied (*apo*-protein), second, when the substrate occupies the binding site, and third, when the drug inhabits the binding site (*holo*-protein). The residue-wise difference in the atomic fluctuations $\Delta RMSF_{(apo-substrate)}$ is obtained by subtracting the atomic fluctuations (RMSF) due to substrate binding from

those observed in the *apo*-protein (see the first term in **Eq 2a**). This identifies residues that interact with the substrate. Similarly, $\Delta RMSF_{(apo\text{-}drug)}$ detects residues that interact with the drug molecule. Finally, $\Delta RMSF_{(substrate\text{-}drug)}$ identifies residues that are critical for either drug or substrate binding (see the first term in **Eq 2b**); and is computed by subtracting the atomic fluctuations due to drug binding from those observed due to substrate binding. Thus, the ΔRMSF values are very helpful in identifying residues critical in the binding of various ligands. However, it suffers from the limitation that it conveys nothing about how the wild-type residue is likely to be substituted by other residues. To do so, we compute the positional variability in the protein using Wu-Kabat's coefficient of variability (**Eq 1**) from multiple sequence alignment (MSA) of homologous proteins.

The ΔFV scores are the product of ΔRMSF and positional variability (**Eqs 2a** and **b**) and are to be interpreted as follows. A positive value for the ΔFV_1 score indicates that the position is affected by ligand binding, whereas zero or a negative value depicts that the position may not be affected by a ligand. The magnitude of ΔFV_1 is larger if the amino acid position is variable, and smaller if it is conserved. Hence, a large ΔFV_1 indicates that a residue is important for ligand binding and has the potential to be substituted. To stress the difference between substrate and drug binding, the ΔFV_2 score has been introduced. If an amino acid position is more important for substrate binding than drug binding, ΔFV_2 is negative, and positive otherwise. The magnitude of ΔFV_2 is again modulated by the position being variable (larger values) or conserved (smaller values). Hence, a large positive ΔFV_2 indicates that a residue is important for drug binding and has the potential to be substituted. Therefore, for a position to be a mutational hotspot leading to drug resistance but not interfering with substrate binding, both ΔFV_1 and ΔFV_2 must have a positive value. Furthermore, the ΔFV scores can be useful in structure-based

drug design to specifically target amino acid residues involved in substrate binding to minimize the chances of drug resistance. For this, positions should be selected that show positive values for ΔFV_1 for the substrate and negative values for ΔFV_2.

Two pitfalls immediately discernible: first, this method is sensitive for amino acid positions that are in direct contact (within ~5 Å) with the drug/substrate. By contrast, amino acid substitutions that are further away from the binding site will suffer from small ΔRMSF values due to the lack of immediate interaction with the drug/substrate. Substitutions at such positions may still lead to resistance through allosteric effects but are hard to predict with the current method. Finally, there are no provisions in the present dispensation to address amino acid substitutions at more than one position.

Wu-Kabat's coefficients based on HHBLITS-generated MSA show that most of the positions known to yield resistance are not well conserved.

Before we discuss the outcome of the ΔFV scores, we evaluate the ability of its components, namely the positional variability and the difference in the atomic fluctuations, to enable us to investigate amino acid conservation and identify amino acid positions that interact with drug/substrate, respectively. **Figure 1** displays the positional variability for HIV-1 protease (single substitutions) leading to drug resistance to any protease inhibitor reported in the HIVdb(36,37) and also for the anaplastic lymphoma kinase inhibitor- crizotinib.

We classify each position in one of three categories based on their amino acid variability – conserved (Wu-Kabat's coefficient of variability < 20), not conserved (> 20), and highly variable (> 40) (**Table S2** Supplementary Section and **Figures 1A** and **1B**). Further, we examine the computed positional variabilities for HIV-1 protease, including the residues involved in catalysis - D25(D25')-T26(T26')-G27(G27') (primed residues belong to chain B of HIV-1 protease).

Since D25-T26-G27 are catalytically essential residues, their substitution with any other amino acid will most likely result in an enzyme with compromised catalytic efficiency. This is exemplified by a high frequency (~81%) of these wild-type residues, therefore categorised as conserved positions. However, Wu-Kabat's coefficient of variability for D25 is 22.23, for T26 19.66 and G27 14.57. Therefore, based on our criteria, D25 must be classified as not conserved, whereas T26 and G27 are labelled as conserved positions. The Wu-Kabat's coefficient of variability (**Eq 1**) is not only sensitive to the frequency of wild-type residues but also to the number of different types of amino acids that occur in the multiple sequence alignment at a particular position in the sequence. In the case of D25, 17 different amino acids are found to substitute the wild-type residue, while it is 15 substitutions for T26, and 11 for G27. Further, we also observe that L23 and L24, where accessory substitutions cause resistance to protease inhibitors, were identified as conserved positions (Supplementary **Table S3A**). This is attributed to the high frequency (~80%) of occurrence of the wild-type residue. Overall, the Wu-Kabat's coefficient of variability computed using HHBLITS-driven multiple sequence alignment (MSA) classifies 26 out of 28 positions (**Tables S3A** and **S3B** and **Supplementary Note 1**) known to cause resistance as not conserved, with two false negative cases (L23 and L24) and one false positive case (D25). Furthermore, in the case of anaplastic lymphoma kinase, all amino acid positions where substitutions occur are highly variable (**Figures 1C and 1D**). Wu-Kabat's coefficients based on HHBLITS-generated MSA show that most of the positions known to yield resistance are not well conserved, which is consistent with the results reported by Kollman *et al*(13).

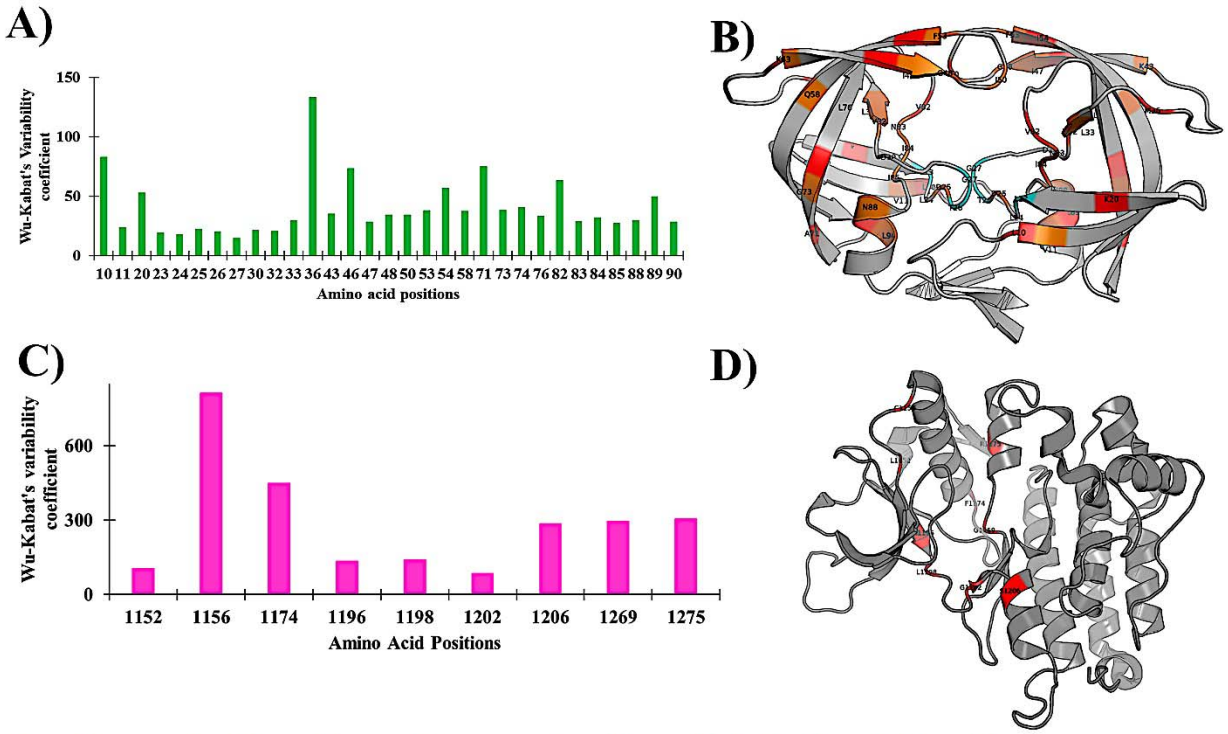

Cyan- Conserved positions; Orange- Not conserved positions; Red- Highly variable positions

Figure 1. Amino acid variability for HIV-1 protease (for all positions reported in the HIV DB leading to drug resistance to any protease inhibitor reported) and anaplastic lymphoma kinase. **A)** Positional variability computed using HHBLITS (green) for HIV-1 protease. **B)** Depiction of substitution positions on the structure of the protease along with their variability computed using Wu-Kabat's coefficient of variability on MSA generated by HHBLITS. **C)** Positional variability computed using HHBLITS (pink) for anaplastic lymphoma kinase. **D)** Depiction of substitution positions on the structure of the anaplastic lymphoma kinase along with their variability computed using Wu-Kabat's coefficient of variability on MSA generated by HHBLITS. In **B**) and **D**) The cyan-coloured residues have Wu-Kabat's variability < 20 (conserved position), orange-coloured residues have Wu-Kabat's variability > 20 (not conserved position), and red-coloured residues have Wu-Kabat's variability > 40 (highly variable position).

ΔRMSF values are indicators of protein-ligand interactions

There are 18 and 10 positions where substitutions have led to resistance to nelfinavir and darunavir respectively (Supplementary **Tables S3A** and **S3B**). Here, we probe if the parameter, ΔRMSF, can be used to identify residues that show strong/weak interaction with the drug/inhibitor in question. We only consider positions in the active site of HIV-1 protease within a 5 Å radius from the ligand nelfinavir or darunavir. If an amino acid lies outside this region, the

ΔRMSF values are not reliable to ascertain whether the changes in the atomic fluctuations are due to the strength of ligand binding. We then test if there is a relation between the change in mobility of the amino acid and the type of substitution observed i.e., accessory substitution or major substitution, that causes resistance to protease inhibitors. Accessory substitutions do not directly influence the binding of drugs, at least for those considered in this study, however, they are known to improve the stability of the enzyme or compensate for lethal amino acid substitutions(36).

For nelfinavir, positions M46, I54, N88, and L90, which carry substitutions that give rise to drug resistance, lie outside the active site region (Supplementary **Tables S3A** and **S3B**). Substitutions at M46(M46') have led to resistance to the protease inhibitors because of an increase in the catalytic efficiency, but do not affect inhibitor binding(38–41). Furthermore, substitutions at L90(L90') are known to reduce the stability of HIV-1 protease(42), which is often compensated for by other substitutions for example, substitutions at N88(43). Since these mutations lie outside the active site region and do not perturb nelfinavir binding directly, it is beyond the scope of the ΔFV score to show reliable predictions, and therefore, these substitutions will not be looked at further.

We note that the probability of side-chain atoms to be found within the active site region is higher than that of backbone atoms (Supplementary **Tables S4A** and **S4B**). Therefore, we use ΔRMSF values of side-chain atoms to compute the ΔFV score.

We evaluate the ability of $\Delta RMSF_{(apo–drug)}$ and $\Delta RMSF_{(substrate\text{-}drug)}$ (**Figures 2A** and **2C**) to identify residues that are more critical for drug binding than for substrate binding, which makes them amenable to substitutions that perturb the binding of inhibitors, thus leading to resistance. $\Delta RMSF_{(apo–drug)}$ values indicate that D25(D25'), T26(T26'), G27(G27'), D30', I47(I47'),

G48(G48'), V82', and I84' lose mobility upon binding of nelfinavir. It can, therefore, be summarised that $\Delta RMSF_{(apo–drug)}$ can identify all 8 amino acids that interact with nelfinavir which lie in the active site, and thus susceptible to mutation. Positive $\Delta RMSF_{(substrate–drug)}$ values suggest that these 8 amino acid residues (including the catalytic residues) become less mobile in the presence of nelfinavir compared to the substrate, suggesting they show more pronounced interactions with the drug. Nelfinavir shows more prominent interactions with residues in chain B, with exceptions of I47 and G48 where the interactions occur with these residues in both chains A and B. Nelfinavir makes strong interactions with the catalytic residues (D25, T26, and G27), where substitutions are lethal for the virus itself. This is a consequence of the structural design strategies of protease inhibitors directed in such a way that strong interactions with the catalytic residues occur for efficient inhibition.

Additionally, we investigate 7 amino acid residues (**Table S5A** in Supplementary information) within the active site of nelfinavir, where no substitutions have been reported so far, using $\Delta RMSF_{(apo–drug)}$ values. The $\Delta RMSF_{(apo–drug)}$ values suggest that all 7 amino acids interact with nelfinavir, and more so with these residues in chain B than chain A. However, the $\Delta RMSF_{(substrate–drug)}$ values suggest that 5 (D29, T31, G49, T80 and P81) of these amino acids show more prominent interactions with the substrate than with nelfinavir. Therefore, they should be less prone to substitutions leading to resistance to nelfinavir.

In the case of darunavir, the $\Delta RMSF_{(apo–drug)}$ values suggest that 7 (Supplementary **Table S3B**) amino acids are known to cause major resistance (**Figures 2B** and **2D**). Darunavir interacts with I47, I50, L76, and V82 in both chains as seen in X-ray crystallography(44). Furthermore, darunavir interacts only with V32' and I84 in chains B and A respectively. The $\Delta RMSF_{(apo–drug)}$ values are in line with X-ray crystallographic observations. We also evaluate the capability of

$\Delta RMSF_{(substrate\text{-}drug)}$ to identify amino acid positions that show more prominent interactions with darunavir than the substrate. We analyse the 6 amino acids (**Figure 3B**) within the active site known to cause resistance to darunavir. The $\Delta RMSF_{(substrate\text{-}drug)}$ values suggest that all positions analysed interact more prominently with darunavir than with the substrate. Thus, we establish that $\Delta RMSF_{(substrate\text{-}drug)}$ is efficient enough to identify the residues that interact more prominently with the drug and substitutions at these sites are likely to cause drug resistance.

Further, we investigate the performance of $\Delta RMSF_{(apo–drug)}$ and $\Delta RMSF_{(substrate\text{-}drug)}$ to identify the propensity for mutation for 10 positions (**Figures 3A** and **3B**) within the active site region of darunavir. Of the 10, three are catalytic residues and for the remaining 7 positions, no substitutions leading to resistance have been reported so far (**Table S5B** Supplementary information). The $\Delta RMSF_{(apo–drug)}$ values suggest that 8 (R8, D25, T26, G27, D29, G49, T80 and P81) out of the 10 residues interact with darunavir. $\Delta RMSF_{(substrate\text{-}drug)}$ values suggest that 7 (R8, G27, D29, T31, G49, T80 and P81) out of the 10 amino acids show more prominent interactions with darunavir than the substrate Therefore, R8, G27, D29, T31, G49, T80 and P81 are amino acid positions more likely to show drug resistant mutations against darunavir.

It is now established, at least for the systems considered in this study, that $\Delta RMSF_{(apo–drug)}$ and $\Delta RMSF_{(substrate\text{-}drug)}$ are good metrics to identify residues that interact with drugs and are good indicators of the tendency of amino acids to undergo mutation. Therefore, they have been employed as components of ΔFV_1 and ΔFV_2 scores.

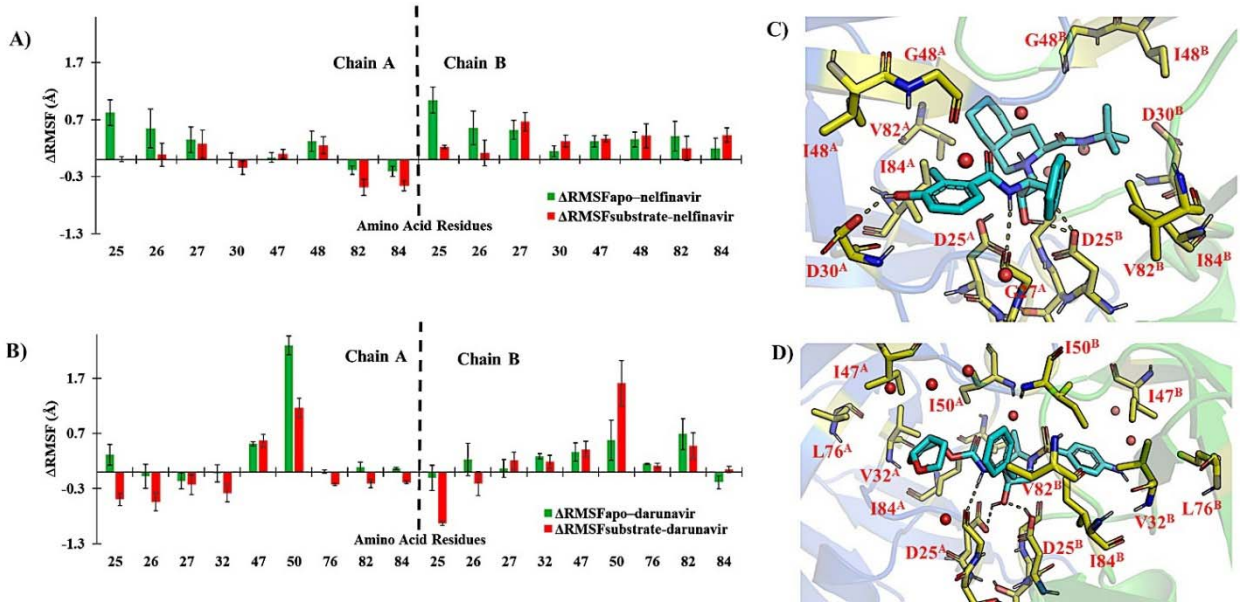

Figure 2. ΔRMSF values (mean ± SEM, n = 3) computed for HIV-1 protease side-chain atoms in the presence of **A)** nelfinavir and **B)** darunavir. **C)** Direct interactions observed in X-ray crystallography of nelfinavir (cyan colour) with HIV-1 protease residues. **D)** Direct interactions observed in X-ray crystallography of darunavir (cyan colour) with HIV-1 protease residues. Blue-coloured cartoons indicate chain A, green-coloured cartoons indicate chain B, red spheres depict water molecules, and yellow dotted lines indicate hydrogen bonds.

Δ*FV scores for HIV-1 inhibitors*

The ΔFV score is the product of positional variability and ΔRMSF. While the sign of the score is influenced by ΔRMSF, the magnitude is dictated by both positional variability and ΔRMSF. This is to say, larger values of ΔFV scores most often signify that the position is not well conserved, and therefore vulnerable to substitution by other amino acids. Furthermore, HIV-1 protease is a symmetric enzyme, however, the inhibitors considered in this work bind asymmetrically, which means the inhibitors show a greater number of interactions which one of the chains of this homodimer. Therefore, ΔFV has been computed for positions on both chains separately; however, for our predictions, only a higher value amongst the two has been considered (**Figure 3**). To investigate the performance of ΔFV scores, we group the amino acid positions into three categories **(Figure 3**), (i) positions within the active-site region known to

mutate leading to major drug resistance, (ii) catalytic residues where mutations are known to directly affect the enzyme efficiency and (iii) positions in the active site for which no resistance cases having been reported for the drugs considered in this study. In the case of nelfinavir, ΔFV_1 (**Figure 3A**) shows that all 5 amino acids (D30, I47, G48, V82, I84) that are known to cause resistance, show a positive score that signifies these positions interact with the drug. The ΔFV_1 scores computed for the catalytic positions (**Figure 3A**) show that all 5 positions (D30, I47, G48, V82, I84)) exhibit direct contact with nelfinavir and this is consistent with the X-ray crystallographic data. For positions where no resistance has been reported, ΔFV_1 scores show that all these amino acids physically interact with the protease, and therefore are prone to mutate with nelfinavir, which is also consistent with X-ray crystallographic data(45). The ΔFV_2 scores show that all 5 amino acids (D30, I47, G48, V82, I84) are mutational hotspots. Furthermore, the ΔFV_2 scores suggest that even the catalytic residues show a positive value, however, these positions are well conserved, and therefore, not susceptible to mutations. Therefore, the predictions for these catalytic residues are considered false positives. Moreover, for positions (R8, A28, D29, T31, G49, T80, P81) there are no reports as on date that indicate any resistance to nelfinavir (except T80 and P81), show positive values for ΔFV_2 which suggests that these positions are prone to mutations. However, the likelihood of R8, A28 and D29 to mutate is low as these positions are fairly conserved with Wu-Kabat's variability coefficient of 19.0, 17.1 and 18.76 respectively. On the other hand, G49 is seemingly a good candidate for mutation as the Wu-Kabat's variability coefficient (26.17) suggests that this position is not conserved. A large positive value for ΔFV_2 (27.74) shows that mutation at this position is likely to cause resistance to nelfinavir.

In the case of darunavir, the ΔFV_1 scores show that all amino acids (see **Figure 3B**) directly interact with darunavir. For the catalytic residues, ΔFV_1 shows that all catalytic residues interact directly with darunavir, however, mutations to these residues will likely be lethal to the virus itself. For positions where no resistance cases have been reported, R8, D29, G49, T80 and P81 are seen to interact with darunavir. The ΔFV_2 scores for positions reported to show major resistance to darunavir were predicted to be hotspots for mutations. For the catalytic residues, two out of three amino acids have been identified as non-mutable or mutation with low probability and G27 is falsely classified as positive. Furthermore, for the amino acids where no resistance has been reported, the ΔFV_2 scores indicate that R8, G49, T80 and P81 are more likely to mutate leading to resistance to darunavir.

Therefore, we can conclude that the ΔFV_2 score offers a good indication of amino acids within the active-site region that are prone to mutation, leading to drug resistance.

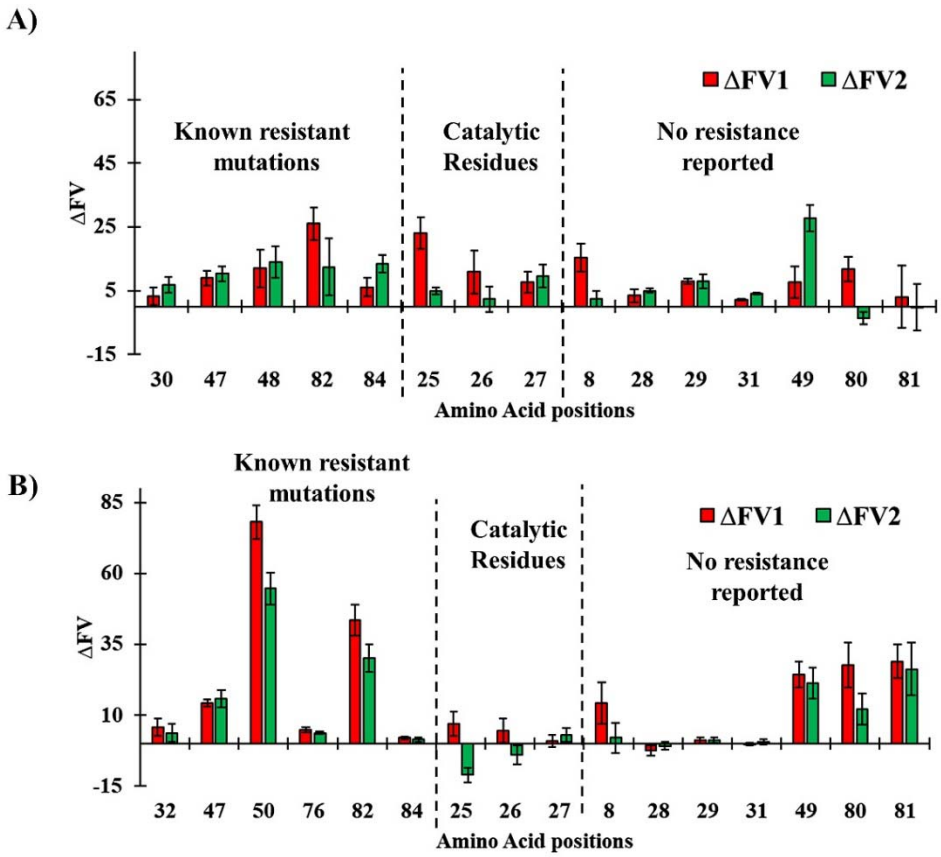

Figure 3: Graphical representation of ΔFV scores for **A)** nelfinavir and **B)** darunavir

ΔFV scores for anaplastic lymphoma kinase inhibitor

As was previously established for the HIV-1 protease system, the differences in the side-chain atomic fluctuations (**Figure 4A**) are more pronounced than those of the backbone fluctuations, and therefore, we use for our analysis atomic fluctuations for side-chain atoms.

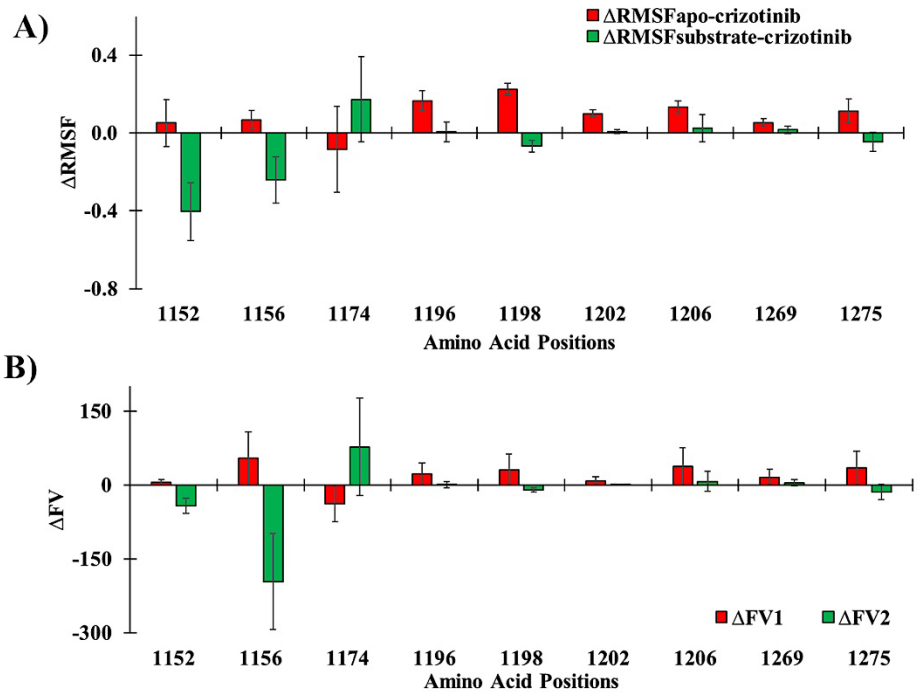

Figure 4. A) ΔRMSF values computed using the side-chain atoms of the ALK kinase domain and **B)** Graphical representation of ΔFV scores for crizotinib.

Since crizotinib is a competitive inhibitor which occupies the same binding site as ATP, the ΔRMSF suggests that ATP and crizotinib have a similar binding pattern with differences observed at L1152 and C1156. The current method shows (**Figure 4B**) only ~38% prediction accuracy in identifying mutational hotspots for crizotinib. This is attributed to the fact that most of the mutations leading to resistance to crizotinib lie outside the active-site region (L1152, C1156, R1275 and F1174), and those that lie within the active-site region (e.g., L1196) are known to enhance the catalytic efficiency of ALK without affecting crizotinib binding. Also,

mutations at C1156, F1174, and R1275 are known to increase the ALK function instead of affecting crizotinib binding. This method shows that only G1202, S1206 and G1269 are likely to cause perturbations in the crizotinib binding which is consistent with previous reports(46,47). Moreover, it has been reported that the L1198F mutant is sensitive to crizotinib(48) and this method shows a negative prediction for this position based on the side chain data. The current method is nonetheless able to identify those residues (G1202, S1206 and G1269) which affect crizotinib binding and the residues that do not influence its binding are predicted negatively, which is to be expected.

CONCLUSIONS

This work describes the development of an empirical score (ΔFV) to identify mutational hotspots. The method combines evolutionary information with binding information at the residue level(10,11). However, to the best of our knowledge this is the first method in the structure-based class of methods that do not use free-energy changes as a measure to identify important amino acid residues involved in drug binding. Moreover, the method makes use of the best-in-class method i.e., the hidden Markov models (HMM), which is based on multiple sequence alignment, to compute the amino acid variability at each position. It has been well established that mutations generally occur at positions with low sequence conservation(10). Such positions have been identified using Wu-Kabat's coefficient of variability. The change in the atomic fluctuations, when different ligands (substrate or drug) occupy the binding pocket, is used to identify crucial residues that are involved in the binding of respective ligands. The residues that interact more prominently with the drug than the substrate are prone to mutate with minimal or no effect on substrate binding, and hence, no compromise in the protein function is expected. Moreover, this information can also be used to design molecules which specifically

show strong interaction with residues that are involved in the substrate binding, leading to a lower possibility of mutations, and thus, resistance can be delayed significantly ("substrate envelope hypothesis").

The ΔFV score developed here is the product of Wu-Kabat's coefficient of variability and atomic fluctuations. Using this score, mutational hotspots have been identified for two FDA approved drugs against HIV-1 protease, namely nelfinavir and darunavir. This method is promising as it could identify almost all mutations that cause major resistance to darunavir and nelfinavir. Further, this method was tested on crizotinib which inhibits human anaplastic lymphoma kinase, which is a difficult target to study, as most of the mutations show complicated mechanisms of drug resistance. In this case, the method could identify 3 positions as mutational hotspots as most mutations either occur outside the active site region or enhance the catalytic efficiency without affecting crizotinib binding. However, we believe that this method has the potential to identify mutational hotspots in the active site region and suggest mutations that have not been observed as yet, in the clinic. This approach can act as a primary screen owing to its computational simplicity and speed, compared to the structure-based methods that employ free-energy computations to identify mutational hotspots. As a primary screen, this approach can help narrow down the choices of positions and amino acid substitutions to be considered for computationally demanding methods like free-energy perturbation or thermodynamic integration. In its present dispensation, the method, however, is unable to identify mutations outside the active site region and at positions which also affect substrate binding. Also, this method is unable to identify double and triple mutations, and further developments are underway to overcome these limitations.

ASSOCIATED CONTENT

Contents of Supplementary information

Supplementary notes 1 and 2 provide explanations to supplementary **Tables S3A** and **S3B** and **S4A** and **S4B** respectively.

Table S1: List of X-ray crystal structures along with their accession codes.

Table S2: Classification of amino acid variability.

Table S3A: Drug-resistant mutations reported in the HIVdb for various inhibitors of HIV-1 protease.

Table S3B: Number and type of mutations for protease inhibitors considered in this study.

Table S4A: Backbone atoms that lie within 5 Å of the ligands as seen in the X-ray crystal structures of HIV-1 protease.

Table S4B: Side-chain atoms that lie within 5 Å of the ligands as seen in the X-ray crystal structures of HIV-1 protease.

Table S5A: $\Delta RMSF_{(apo–drug)}$ and $\Delta RMSF_{(substrate\text{-}drug)}$ values computed using side-chain atoms for nelfinavir for non-resistant positions.

Table S5B: $\Delta RMSF_{(apo–drug)}$ and $\Delta RMSF_{(substrate\text{-}drug)}$ values computed using side-chain atoms for darunavir for non-resistant positions.

Figure S1: Cα RMSD and normalized distribution plots for wild-type HIV-1 protease system. A) *Apo* HIV-1 protease, B) Substrate-bound HIV-1 protease, C) Nelfinavir-bound HIV-1 protease, D) Darunavir-bound HIV-1 protease and E) Normalized distribution plot for Cα RMSD. Runs 1, 2 and 3 indicate three independent MD runs.

Figure S2: Cα RMSD and normalized distribution plots for human anaplastic lymphoma kinase (ALK) system. A) *Apo* ALK, B) Substrate-bound ALK, C) Crizotinib-bound ALK, and D) Normalized distribution plot for Cα RMSD. Runs 1, 2 and 3 indicate three independent MD runs.

Figure S3: RMS average correlation (RAC) for HIV-1 protease system **A)** *apo*protein **B)** substrate-bound protein **C)** protease bound with nelfinavir and **D)** protease bound with darunavir.

Figure S4: RMS average correlation (RAC) for human anaplastic lymphoma kinase; **A)** *apo*protein **B)** substrate-bound protein and **C)** Crizotinib-bound protein.

AUTHOR INFORMATION

CORRESPONDING AUTHOR

Elvis A. F. Martis, Molecular Simulations Group, Department of Pharmaceutical Chemistry, Bombay College of Pharmacy, Kalina, Santacruz [E], Mumbai 400098, India. Phone: +91-7506161232. E-mail: elvis.martis@bcp.edu.in

AUTHOR CONTRIBUTIONS

EAF Martis designed and conducted computational studies, EAF Martis and EC Coutinho analysed the data, and EC Coutinho supervised the research and provided computing resources. All authors wrote, reviewed, and approved the draft of the manuscript.

FUNDING SOURCES

This work was supported by a grant from BASF SE, Ludwigshafen am Rhein, Germany to EC Coutinho which includes doctoral funding to EAF Martis.

ACKNOWLEDGEMENTS

EAF Martis and EC Coutinho are grateful to the Department of Science and Technology (DST), Department of Biotechnology (DBT) and Council of Scientific and Industrial Research (CSIR) for their financial support to build the High-Performance Computing system at the Department of Pharmaceutical Chemistry, Bombay College of Pharmacy. EAF Martis and EC Coutinho are recipients of a hardware support grant from NVIDIA Corporation. EAF Martis is indebted to BASF, Ludwigshafen, Germany for a PhD fellowship and the MCBR4 (2015) consortium (Prof. Dr P. Comba, University of Heidelberg; Prof. Dr H. Zipse LMU, Munich and Prof. Dr G. N. Sastry, IICT, Hyderabad for MCBR visiting fellowship to the Heine-Heinrich University of Düsseldorf, Germany under Prof Dr Holger Gohlke). EAF Martis and EC Coutinho are grateful

to Dr. Ian R Craig, computational chemist, BASF, Ludwigshafen, Germany for carefully reading the draft of this manuscripts and providing valuable insights that significantly improved the work described in this work.

References

1. Gulnik SV, Suvorov LI, Liu B, Yu B, Anderson B, Mitsuya H, et al. Kinetic characterization and cross-resistance patterns of HIV-1 protease mutants selected under drug pressure. Biochemistry. 1995;34(29):9282–7.

2. Schliekelman P, Garner C, Slatkin M. Natural selection and resistance to HIV. Nature. 2001;411(6837):545.

3. Toprak E, Veres A, Michel JB, Chait R, Hartl DL, Kishony R. Evolutionary paths to antibiotic resistance under dynamically sustained drug selection. Nat Genet. 2012;44(1):101.

4. Walsh C. Molecular mechanisms that confer antibacterial drug resistance. Nature. 2000;406(6797):775.

5. Longley D, Johnston P. Molecular mechanisms of drug resistance. J Pathol J Pathol Soc G B Irel. 2005;205(2):275–92.

6. Andersson DI, Levin BR. The biological cost of antibiotic resistance. Curr Opin Microbiol. 1999;2(5):489–93.

7. Gagneux S, Long CD, Small PM, Van T, Schoolnik GK, Bohannan BJ. The competitive cost of antibiotic resistance in Mycobacterium tuberculosis. Science. 2006;312(5782):1944–6.

8. Chellappan S, Kairys V, Fernandes MX, Schiffer C, Gilson MK. Evaluation of the substrate envelope hypothesis for inhibitors of HIV□1 protease. Proteins Struct Funct Bioinforma. 2007;68(2):561–7.

9. Nalam MN, Ali A, Altman MD, Reddy GKK, Chellappan S, Kairys V, et al. Evaluating the substrate-envelope hypothesis: structural analysis of novel HIV-1 protease inhibitors designed to be robust against drug resistance. J Virol. 2010;84(10):5368–78.

10. Özen A, Haliloğlu T, Schiffer CA. Dynamics of preferential substrate recognition in HIV-1 protease: redefining the substrate envelope. J Mol Biol. 2011;410(4):726–44.

11. Martis EA, Coutinho EC. Free Energy-Based Methods to Understand Drug Resistance Mutations. In: Structural Bioinformatics: Applications in Preclinical Drug Discovery Process. Springer; 2019. p. 1–24.

12. Cao ZW, Han LY, Zheng CJ, Ji ZL, Chen X, Lin HH, et al. Computer prediction of drug resistance mutations in proteins. Drug Discov Today. 2005;10(7):521–9.

13. Wang W, Kollman PA. Computational study of protein specificity: the molecular basis of HIV-1 protease drug resistance. Proc Natl Acad Sci. 2001;98(26):14937–42.

14. Wang W, Lim WA, Jakalian A, Wang J, Wang J, Luo R, et al. An analysis of the interactions between the Sem− 5 SH3 domain and its ligands using molecular dynamics, free energy calculations, and sequence analysis. J Am Chem Soc. 2001;123(17):3986–94.

15. Frisch M, Trucks G, Schlegel Hb, Scuseria G, Robb M, Cheeseman J, et al. Gaussian 03, revision c. 02; Gaussian. 2004.

16. Besler BH, Merz Jr KM, Kollman PA. Atomic charges derived from semiempirical methods. J Comput Chem. 1990;11(4):431–9.

17. Wang J, Wang W, Kollman PA, Case DA. Automatic atom type and bond type perception in molecular mechanical calculations. J Mol Graph Model. 2006;25(2):247–60.

18. Wang J, Wolf RM, Caldwell JW, Kollman PA, Case DA. Development and testing of a general amber force field. J Comput Chem. 2004;25(9):1157–74.

19. Meagher KL, Redman LT, Carlson HA. Development of polyphosphate parameters for use with the AMBER force field. J Comput Chem. 2003;24(9):1016–25.

20. Wright DW, Hall BA, Kenway OA, Jha S, Coveney PV. Computing clinically relevant binding free energies of HIV-1 protease inhibitors. J Chem Theory Comput. 2014;10(3):1228–41.

21. Yang Z, Lasker K, Schneidman-Duhovny D, Webb B, Huang CC, Pettersen EF, et al. UCSF Chimera, MODELLER, and IMP: an integrated modeling system. J Struct Biol. 2012;179(3):269–78.

22. Jorgensen WL, Jenson C. Temperature dependence of TIP3P, SPC, and TIP4P water from NPT Monte Carlo simulations: Seeking temperatures of maximum density. J Comput Chem. 1998;19(10):1179–86.

23. Darden T, York D, Pedersen L. Particle mesh Ewald: An N· log (N) method for Ewald sums in large systems. J Chem Phys. 1993;98(12):10089–92.

24. Case DA, Cheatham III TE, Darden T, Gohlke H, Luo R, Merz Jr KM, et al. The Amber biomolecular simulation programs. J Comput Chem. 2005;26(16):1668–88.

25. Ryckaert JP, Ciccotti G, Berendsen HJ. Numerical integration of the cartesian equations of motion of a system with constraints: molecular dynamics of n-alkanes. J Comput Phys. 1977;23(3):327–41.

26. Roe DR, Cheatham III TE. PTRAJ and CPPTRAJ: software for processing and analysis of molecular dynamics trajectory data. J Chem Theory Comput. 2013;9(7):3084–95.

27. Remmert M, Biegert A, Hauser A, Söding J. HHblits: lightning-fast iterative protein sequence searching by HMM-HMM alignment. Nat Methods. 2012;9(2):173.

28. Pruitt KD, Tatusova T, Maglott DR. NCBI Reference Sequence (RefSeq): a curated non-redundant sequence database of genomes, transcripts and proteins. Nucleic Acids Res. 2005;33(suppl_1):D501–4.

29. Kabat E, Wu TT, Bilofsky H. Unusual distributions of amino acids in complementarity determining (hypervariable) segments of heavy and light chains of immunoglobulins and their possible roles in specificity of antibody-combining sites. J Biol Chem. 1977;252(19):6609–16.

30. UniProt Consortium. UniProt: a hub for protein information. Nucleic Acids Res. 2014;43(D1):D204–12.

31. Nalam MN, Ali A, Altman MD, Reddy GKK, Chellappan S, Kairys V, et al. Evaluating the substrate-envelope hypothesis: structural analysis of novel HIV-1 protease inhibitors designed to be robust against drug resistance. J Virol. 2010;84(10):5368–78.

32. Chellappan S, Kiran Kumar Reddy G, Ali A, Nalam MN, Anjum SG, Cao H, et al. Design of mutation resistant HIV protease inhibitors with the substrate envelope hypothesis. Chem Biol Drug Des. 2007;69(5):298–313.

33. Chellappan S, Kairys V, Fernandes MX, Schiffer C, Gilson MK. Evaluation of the substrate envelope hypothesis for inhibitors of HIV 1 protease. Proteins Struct Funct Bioinforma. 2007;68(2):561–7.

34. Galindo-Murillo R, Roe DR, Cheatham III TE. On the absence of intrahelical DNA dynamics on the μs to ms timescale. Nat Commun. 2014;5:5152.

35. Galindo-Murillo R, Roe DR, Cheatham III TE. Convergence and reproducibility in molecular dynamics simulations of the DNA duplex d (GCACGAACGAACGAACGC). Biochim Biophys Acta BBA-Gen Subj. 2015;1850(5):1041–58.

36. Chang MW, Torbett BE. Accessory mutations maintain stability in drug-resistant HIV-1 protease. J Mol Biol. 2011;410(4):756–60.

37. Shafer RW. Rationale and uses of a public HIV drug resistance database. J Infect Dis. 2006;194(Supplement_1):S51–8.

38. Schock HB, Garsky VM, Kuo LC. Mutational Anatomy of an HIV-1 Protease Variant Conferring Cross-resistance to Protease Inhibitors in Clinical Trials COMPENSATORY MODULATIONS OF BINDING AND ACTIVITY. J Biol Chem. 1996;271(50):31957–63.

39. Henderson GJ, Lee SK, Irlbeck DM, Harris J, Kline M, Pollom E, et al. Interplay between single resistance-associated mutations in the HIV-1 protease and viral infectivity, protease activity, and inhibitor sensitivity. Antimicrob Agents Chemother. 2012;56(2):623–33.

40. Pazhanisamy S, Stuver CM, Cullinan AB, Margolin N, Rao B, Livingston DJ. Kinetic characterization of human immunodeficiency virus type-1 protease-resistant variants. J Biol Chem. 1996;271(30):17979–85.

41. Piana S, Carloni P, Rothlisberger U. Drug resistance in HIV 1 protease: flexibility assisted mechanism of compensatory mutations. Protein Sci. 2002;11(10):2393–402.

42. Hong L, Zhang XC, Hartsuck JA, Tang J. Crystal structure of an in vivo HIV-1 protease mutant in complex with saquinavir: insights into the mechanisms of drug resistance. Protein Sci. 2000;9(10):1898–904.

43. Mitsuya Y, Winters MA, Fessel WJ, Rhee SY, Hurley L, Horberg M, et al. N88D facilitates the co-occurrence of D30N and L90M and the development of multidrug resistance in HIV type 1 protease following nelfinavir treatment failure. AIDS Res Hum Retroviruses. 2006;22(12):1300–5.

44. Yedidi RS, Maeda K, Fyvie WS, Steffey M, Davis DA, Palmer I, et al. P2′ benzene carboxylic acid moiety is associated with decrease in cellular uptake: evaluation of novel nonpeptidic HIV-1 protease inhibitors containing P2 bis-tetrahydrofuran moiety. Antimicrob Agents Chemother. 2013;57(10):4920–7.

45. Kaldor SW, Kalish VJ, Davies JF, Shetty BV, Fritz JE, Appelt K, et al. Viracept (nelfinavir mesylate, AG1343): a potent, orally bioavailable inhibitor of HIV-1 protease. J Med Chem. 1997;40(24):3979–85.

46. Sun H, Li Y, Li D, Hou T. Insight into crizotinib resistance mechanisms caused by three mutations in ALK tyrosine kinase using free energy calculation approaches. J Chem Inf Model. 2013;53(9):2376–89.

47. Hallberg B, Palmer RH. Mechanistic insight into ALK receptor tyrosine kinase in human cancer biology. Nat Rev Cancer. 2013;13(10):685.

48. Shaw AT, Friboulet L, Leshchiner I, Gainor JF, Bergqvist S, Brooun A, et al. Resensitization to crizotinib by the lorlatinib ALK resistance mutation L1198F. N Engl J Med. 2016;374(1):54–61.